Transitioning with confidence during contact/non-contact scenarios

Seyed Sina Mirrazavi Salehian[1], Hsiu-Chin Lin[2], Nadia Figueroa[1], Joshua Smith[2], Michael Mistry[2], Aude Billard[1]

***Abstract*— In this work, we propose a probabilistic-based approach for detecting transitions in hybrid control systems with limited sensing. Detecting the transition moment is a particularly challenging problem as (i) multiple sources of sensory information are usually not available in robotic systems and (ii) the sensory information is noisy and requires calibrations. The challenge significantly increases if the robot makes physical contact as it causes discontinuities in the dynamics. The proposed transition criterion addresses these shortcomings by studying the behavior of the robot and the environment during a short horizon of time. We empirically validate our approach while detecting contact transitions in a hand-over scenario where a human operator brings a large object and hands it over to a pair of robotic arms which are not equipped with a force or tactile sensors.**

I. Introduction

By leveraging multiple sub-action controllers, humans have demonstrated remarkable capabilities in performing manipulation tasks that require making and breaking contact with objects [1], [2]. In order to confidently transition between these successive sub-action controllers, multiple sources of sensory information, such as tactile, vision or audition, are engaged. Studies have shown that that integrating different source of sensory information reduces ambiguity regarding the environment. This, consequently, improves humans ability in confidently detecting the transition moments [3], [4]. The ultimate goal for robotic platforms is to work in unstructured environments where, just like humans, multiple sub-action controllers are required to accomplish complex manipulation tasks. In such scenarios, detecting the true transitions plays a vital role in the accomplishment of the desired task. Unlike humans, due to hardware limitations, robotic platforms are commonly not equipped with multiple sources of sensory information, e.g., vision, force and tactile sensors. Moreover, sensors are often noisy and require periodic calibration.. Hence, confidently detecting event-based transitions, such as making and breaking physical contact with an object or a surface, is not trivial. A typical scenario is the *contact/non-contact transition*, where the robot switches from free-space motion (non-contact) to constrained motion (contact). During the free motion phase, the *unconstrained motion* controller guides the robot to make a contact with the environment. Once the robot is in contact, the *constrained motion* controller must take over the guidance while controlling for the interaction forces (see Fig. 1).

If force or tactile information is not available, one solution is to switch from one controller to another according to the distance between the robot and the environment. Early approaches on contact transitions adapt the "hybrid systems" approaches [5], [6], which exhibit both continuous and discrete dynamic behaviors. Given perfect knowledge of the robot's position and the environment, these methods can achieve precise force/motion tracking and perform smooth transitions. Such an assumption is hard to meet as a complete representation of the environment is generally unknown or if the sensory signals are subject to noise which can easily lead to unstable behaviors [7], [8]. Moreover, hard switches may lead to an infinite number of discrete transitions between controllers (as known as "chattering") in a finite time [9]. One way to deal with this problem is to apply filtering on the observations [10], but the complexity grows with time. This can also be tackled by approximation over a finite observation [11] and/or estimate of the transition probabilities [12].

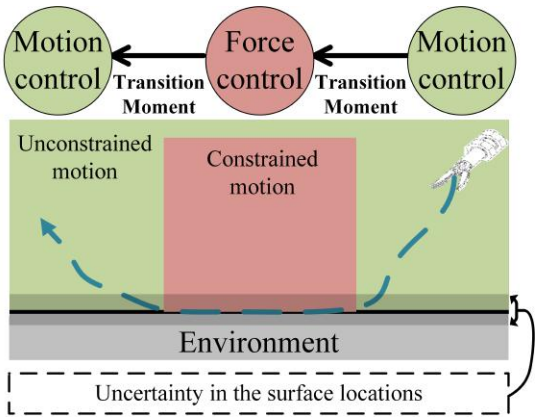

Fig. 1: An illustrative example of dual-phase hybrid controllers. The force control must take over if and only if the robot is in contact with the environment. The transition needs to be detected by measuring the distance between the robot's end-effector and the surface as the robot is not equipped with force or tactile sensors.

Compliant control architectures can address the problem of switching by imitating the behavior of a spring-damper system which is connected between the robot and a target. Some focus on variations of compliant controllers to reduce the impact forces, such as using velocity feedback to improve impact response [13], increasing the velocity gains of the controller for a limited time after impact [14], or avoiding large impact force/velocity during transition [15], [16]. Although these architectures have implicitly addressed the issue of detecting transitions by eliminating the need of switching, they suffer from one shortcoming: they are action-specific. This limits the use of these controllers to broader scenarios where transitions are required across a set of actions or

[1]Learning Algorithms and Systems Laboratory (LASA), Swiss Federal Institute of Technology, Lausanne (EPFL), Switzerland.

[2]Institute of Perception, Action, and Behaviour, School of Informatics, University of Edinburgh, Edinburgh, UK.

control architectures. In this paper, we propose a probabilistic based criterion to detect transitions in hybrid control systems with limited sensing. By using the proposed criterion, we can confidently detect the exact instance in which the systems make contact with an external agent in the face of uncertainty from the measured state of the system or the agent. We have studied the performance of the proposed method in a hand-over scenario where a human operator brings a box and hands it over to a pair of robotic arms that then place it on a desired location.

The rest of the paper is organized as follows. In Section III, we introduce our probabilistic-based approach to indicate the time of transition. In Section IV, we validate the proposed approach in performing a bi-manual object manipulation task.. Discussions and future works are presented in Section V.

II. Problem Formulation

Let us consider systems in the following form

$$\dot{x} = f(x,t) + u(x, x^e, \varphi) \tag{1}$$

where $x,\ x^e \in \mathbb{R}^d$ are the states of the system and the external agent, respectively. For the sake of brevity, apart from these two signals, the rest of the variables are indicated by φ. $u(x, x^e, \varphi) \in \mathbb{R}^d$ is the hybrid control law which is defined with respect to the states:

$$u(x, x^e, \varphi) = \begin{cases} u_1(x, x^e, \varphi) & if \quad \|x - x^e\| \leq \delta \quad (2a) \\ u_2(x, x^e, \varphi) & if \quad \|x - x^e\| > \delta \quad (2b) \end{cases}$$

where $u_i(.),\ \forall i \in \{1, 2\}$ are the desired sub-action controllers and $\delta \in \mathbb{R}^+$ is the threshold for switching between two control laws. In theory, one can switch the control input between Eq. (2a) and Eq. (2b) when $\|x - x^e\| \leq \delta$ and $\|x - x^e\| > \delta$, respectively. However, due to noises in the sensory signals, this distance-based approach suffers from two main shortcomings in practice:

1) Switching between two systems might cause chattering
2) Switching might happen at wrong moments; e.g., $\|x - x^e\|$ is actually greater than δ, however, due to the presence of noise, it is perceived less than δ.

To address these shortcomings, we propose a probability-based criterion to confidently detect the transition moment.

III. Transition with confidence

Let $x(x^e), \hat{x}(\hat{x}^e)$ be the measured and the true states of the system (agent) subject to Gaussian noise $\epsilon(\epsilon^e) \sim \mathcal{N}(0, \Sigma(\Sigma^e))$ such that $x = \hat{x} + \epsilon$ and $x^e = \hat{x}^e + \epsilon^e$. The Euclidean distance between x and x^e can be described as:

$$\|\tilde{x}\| = \|x - x^e\| = \|\hat{x} - \hat{x}^e + \epsilon - \epsilon^e\| \tag{3}$$

Assuming that u_1 is a control law that generates the motion of the robot constrained by a surface and it is crucial to ensure that (2a) is solely activated when $\|\hat{x} - \hat{x}^e\| \leq \delta$; i.e. once the robot is in contact. To ensure this, we can approximate (3) by its upper bound;[1] i.e.

$$\|x - x^e\| = \|\hat{x} - \hat{x}^e\| + \|\tilde{\epsilon}\| \tag{4}$$

where $\|\tilde{\epsilon}\| = \|\epsilon - \epsilon^e\|$. Assuming the noises along all axes are independently and identically distributed, $\|\tilde{\epsilon}\| = \sqrt{\sum_{i=1}^{d} (\tilde{\epsilon}_i)^2}$ forms a d degree-of-freedom Chi distribution with

$$\begin{aligned} E(\|\tilde{\epsilon}\|^2) &= \tilde{\Sigma}^{-2} E(\chi(d)) \\ Var(\|\tilde{\epsilon}\|^2) &= \tilde{\Sigma}^{-4}(d - E(\chi(d))) \end{aligned} \tag{5}$$

With respect to this and as $\hat{x}$ and $\hat{x}^e$ are independent from noise signals, one can calculate the mean $(\tilde{\mu})$ and the variance $(\tilde{\Sigma})$ of $\|\tilde{x}\|$ as follows:

$$\tilde{\mu} = E(\|\hat{x} - \hat{x}^e\|) + \tilde{\Sigma}^{-2} E(\chi(d)) \tag{6a}$$

$$\tilde{\Sigma} = Var(\|\hat{x} - \hat{x}^e\|) + \tilde{\Sigma}^{-4}(d - E(\chi(d))) \tag{6b}$$

The probability that the true distance between the system and and agent is less than or equal to the threshold value δ is

$$P(\|\hat{x} - \hat{x}^e\| \leq \delta; \tilde{\mu}, \tilde{\Sigma}) \tag{7}$$

Since we have no statistical assumption on $\tilde{x}$, the probability distribution (7) is an unknown distribution. However, in the contact/non-contact scenarios, the motion of the system is constrained by the agent once the system is in contact with it. Assuming that the agent does not deform, $\|\hat{x} - \hat{x}^e\|$ can be assumed constant for a given T_k observations. By this, one can approximate (7) by using the Chi or normal distributions for small or large d, respectively[2]. We thus propose to estimate the probability of $\|\hat{x} - \hat{x}^e\| \leq \delta$ as follows:

$$P(\|\hat{x} - \hat{x}^e\| \leq \delta; \underbrace{\bar{\mu}, \bar{\Sigma}}_{\bar{\theta}}) \in [0, 1] \tag{8}$$

where $\bar{\mu}$ and $\bar{\Sigma}$ are the mean and the variance of the Euclidean distance between the states of the system and the agent over T_k step-time. Note that, the probability density function defined by (8) tends toward zero or one if $\hat{x}$ and $\hat{x}^e$ are far from or very close to each other, respectively. Once $P(\|\hat{x} - \hat{x}^e\| \leq \delta; \bar{\theta}) \approx 1$, one can confidently say $\|\hat{x} - \hat{x}^e\| \leq \delta$ and thus, it is the right time to switch (2b) to (2a). Hence, (8) improves the performance of the switching controller as (i) the chattering on the decision boundary is avoided and (ii) the controller switches at the right time. Given criterion (8), the control law (2a) and (2b) can be re-written as:

$$u(x, x^e, \varphi) =$$

$$\begin{cases} u_1(x, x^e, \varphi) & \text{if } P(\|\hat{x} - \hat{x}^e\| \leq \delta, \bar{\theta}) \leq \delta_p \quad (9a) \\ u_2(x, x^e, \varphi) & \text{if } P(\|\hat{x} - \hat{x}^e\| \leq \delta, \bar{\theta}) > \delta_p \quad (9b) \end{cases}$$

[1] Noteworthy is that, if (2b) shall not be activated when $\|\hat{x} - \hat{x}^e\| \leq \delta$, can be approximated by its lower bound, which is $\|\hat{x} - \hat{x}^e\| - \|\tilde{\epsilon}\|$.

[2] Based on the central limit theorem, a chi distribution converges to a normal distribution for sufficiently large degrees of freedom [17].

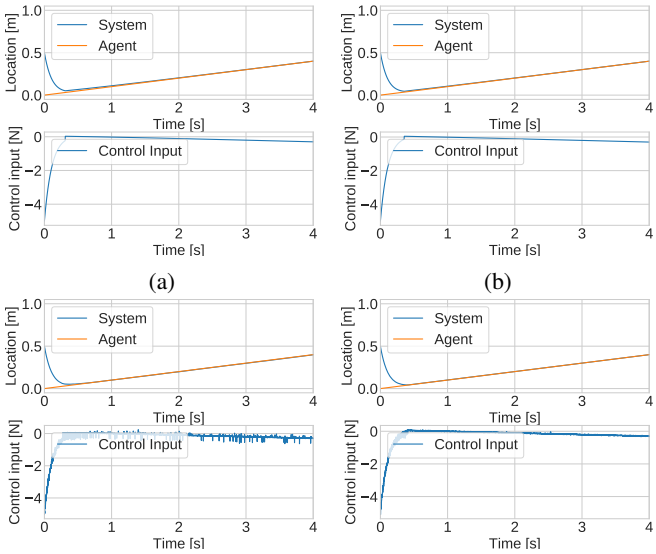

Fig. 2: Fig. 2a and Fig. 2b illustrate the behavior of the system controlled by (2) and (9) in non-noisy environment, respectively. In Fig. 2a and Fig. 2b, the system is controlled by (2) and (9), respectively. $\Sigma = \Sigma^e = 0.007$ and $T_k = 30$. In this example, as $d = 1$, we approximate (8) by a Chi distribution: $P(\|\hat{x} - \hat{x}^e\| \leq \delta; \bar{\theta}) = \chi(|\hat{x} - \hat{x}^e| \leq \delta, \bar{\theta})$.

where $0 < \delta_p < 1$ defines the level of confidence. Based on the central limit theorem, the mean of the distance convergences to the true expected value for sufficiently large horizon time. However, defining T_k is closely related to the rate of changes of $\|\hat{x} - \hat{x}^e\|$. If the rate is high, T_k should be defined small such that (8) can be approximated with normal/chi distributions. However, this comes with the cost of inaccuracies in calculating the true expected value. On the contrary, if the rate is low, T_k can be large enough to be able to approximate (8) with a normal distribution. Based on our experiments, a good rule of thumb is that d and T_k are large if $50 \leq T_k d$.

Example Consider the following system and agent.

$$\dot{x} = x + u, \qquad x(0) = 0.1 \tag{10}$$

$$\dot{x}^e = 0.1, \qquad x^e(0) = 0 \tag{11}$$

with $u_1 = -10x + 9x^e + 0.1$, $u_2 = -2x + x^e$ and $\delta = 0.02$. As it has been shown in Fig. 2a and Fig. 2b, if the measurements are not noisy, both (2) and (9) result in the same behavior. However, if the measurements are noisy, (2) causes chattering while (9) results in smooth control inputs; compare Fig. 2c with Fig. 2d.

IV. Empirical validation

The practicality of the proposed approach is validated on a real-world scenario. We consider a system with $d = 6$ degree-of-freedom and $T_k = 15$ observations. The observed state of the system is subject to some Gaussian noise, and the norm of the noise forms a Chi-distribution defined in (8). As $50 < dT_k$, the probability function (8) is approximated by a normal distribution.

In this scenario, we consider the case where a human operator brings a large object (a box) and hands it over to a pair of robotic arms that is then placed on a desired location; see Fig. 3. The proposed framework is implemented on a real dual-arm platform, consisting of two 7 DOF KUKA LWR 4+. The robots are controlled via Fast Research Interface (FRI) at 1000Hz. The position of the object is captured by the Optitrack motion capture system from Natural Point at 240 Hz.

The dynamic equation of i^{th} robotic manipulator with N_i revolute joints can be described by the following second-order nonlinear differential equation:

$$M_i(q_i)\ddot{q}_i + h_i(q_i, \dot{q}_i) = \tau_i + J_i(q_i)^T F_{c_i} \tag{12}$$

where $q_i \in \mathbb{R}^{N_i \times 1}$ is the joint positions, $M_i(q_i) \in \mathbb{R}^{N_i \times N_i}$ is the Inertia matrix, $h_i(q_i, \dot{q}_i) \in \mathbb{R}^{N_i \times 1}$ is the Coriolis, Centrifugal and Gravitational force vector, $J_i(q_i) \in \mathbb{R}^{6 \times N_i}$ is the Jacobian that relates the joint space to the point of contacts, $\tau_i \in \mathbb{R}^{N_i \times 1}$ is the control torque, $F_{c_i} \in \mathbb{R}^{6 \times 1}$ is contact forces between the robot and the environment, and the subscript i denotes the i^{th} manipulator. By concatenating the dynamic equation (12) $\forall i \in \{1, 2\}$, the dynamic of the robotic system in a compact form as follows:

$$M(q)\ddot{q} + H(q, \dot{q}) = \tau + J_c(q)^T F_c \tag{13}$$

where $\tau = \begin{bmatrix} \tau_1 & \tau_2 \end{bmatrix}^\top$ is the joint torques of the two arms. In order to successfully perform this task, the following subtasks need to be accomplished

- **Free space phase**: During the free space phase, the aim of the robots is to reach the moving object and grab it from the desired grabbing points. To this end, the motion of the robotic arms must be coordinated with each other and with the moving object such that both of them intercept the object and grab it from the desired locations. As the arms' motion must be continuously updated in synchrony to adapt to the changes in the objects trajectory, we use the virtual object based motion planning approach for controlling the robots' motions during the *free space* phase [18], [19]. The control architecture $u_2(x, x^e, \varphi)$ for the *free* phase is presented in Appendix A.
- **Contact phase**: During the contact phase, the aim of the robots is to place the grabbed object at a desired location while being robust to external disturbances. To this end, the interaction/contact forces need to be precisely controlled such that the robots can perform the task while being compliant to external disturbances., yet maintaining firm grasps of the object. Moreover, the robots must maintain enough contact force so the object does not slip on the box, and the force exerted by the robots must not damage the object. To achieve these two objectives, we use the projected inverse dynamic approach for controlling the multi-arm grasping proposed in [20]. The control architecture $u_1(x, x^e, \varphi)$ for the *contact* phase is presented in Appendix B.

The robot must switch from the *free space* phase controller $u_2(x, x^e, \varphi)$ to the *contact phase* controller $u_1(x, x^e, \varphi)$ once it is in contact with the object. As the robotic arms are not equipped with any force/torque sensors, the only way to

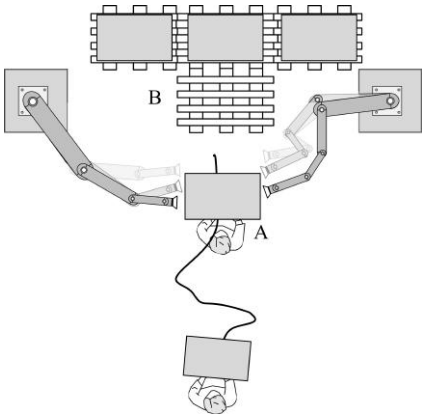

Fig. 3: Illustration of Dual-arm Task-Space Coordination. The goal of the task is to grab the object and place it at the desired location.

detect the contact is by calculating the distance between the robots' end-effectors and the desired grabbing positions on the object. Hence, the proposed hybrid system (9) is used to switch confidently from the *free space* phase controller to the *contact phase* controller.

As the contact space controller must be activated if and only if the robots have reached the desired grabbing locations, we set $\delta_p = 0.99$. When the operator carrying the box approaches the robots, the virtual object and coordinately the robots, reach the box and follow it till they intercept the object at the desired grabbing points. Once, the robots are in contact with the object, the probability function $P(\|\hat{x} - \hat{x}^e\| \leq \delta, \bar{\theta})$ increases towards one and the *contact phase* control law takes over. As it can be seen in the accompanying video and Fig. 4, this transition is smooth and the robots stay in contact with the object afterwards. At the end of the scenario, the object is placed at the desired location on the table. An example of the motion of the arms, the object and the probability of being in contact are shown in Fig. 5.

V. Summary and Discussion

In this paper, we proposed a probabilistic-based criterion to confidently detect transitions in hybrid control systems with limited sensing. This criterion improves the robustness of the controller in the face of noisy signals and uncertainties by studying the distance between the system and the agent for a time horizon. The performance of the proposed criterion is verified in a real-world scenario where the measurements are noisy.

In contact/non-contact scenarios, the motion of the system is constrained by the agent once it is in contact with the agent. We leverage this property and approximate the probabilistic criterion by Normal or Chi distributions by assuming that the distance between the system and the agent is constant for a time horizon. Even though this cannot be generalized for free-space motions, one can assume that the distance is constant for a short time horizon if the sampling frequency is much higher than the speed of the system and the agent. It is noteworthy that if none of these assumptions are true, one cannot approximate (8) by normal distributions. In future works, we are planning to relax these assumptions and study the cases where the motion of the agent/system are faster than the sampling rate.

In this paper, the distance between the system and the agent is calculated in Euclidean space. This can also be generalized for other distance functions as long as the function is strictly monotonic.

As the main scope of this paper is detecting the true transition time and not the stability of the multi-phase hybrid systems, we have not studied the stability of (1) controlled by (9). The ongoing work is oriented towards detecting transitions while ensuring the stability of hybrid systems.

Acknowledgement

This paper was partially supported by the European Commission, within the CogIMon project in the Horizon 2020 Work Programme (ICT-23-2014, grant agreement 644727) and Crowdbots (ICT-25-2016-2017).

References

[1] J. R. Flanagan, M. C. Bowman, and R. S. Johansson, "Control strategies in object manipulation tasks," *Current Opinion in Neurobiology*, vol. 16, no. 6, pp. 650 – 659, 2006, motor systems / Neurobiology of behaviour.

[2] R. S. Johansson and K. J. Cole, "Sensory-motor coordination during grasping and manipulative actions," *Current Opinion in Neurobiology*, vol. 2, no. 6, pp. 815–823, 1992.

[3] M. O. Ernst and H. Bulthoff, "Merging the senses into a robust percept," *Trends in Cognitive Sciences*, vol. 8, no. 4, pp. 162–169, 2004.

[4] L. Biel and P. Wide, "An intelligent model approach for combination of sensor information," 2002, pp. 43–47, cited By 1.

[5] M. H. Raibert and J. J. Craig, "Hybrid position/force control of manipulators," *Journal of Dynamic Systems, Measurement, and Control*, vol. 103, no. 2, pp. 126–133, 1981.

[6] D. J. F. Heck, A. Saccon, N. van de Wouw, and H. Nijmeijer, "Switched position-force tracking control of a manipulator interacting with a stiff environment," in *2015 American Control Conference (ACC)*, July 2015, pp. 4832–4837.

[7] M. S. Branicky, "Multiple lyapunov functions and other analysis tools for switched and hybrid systems," *IEEE Transactions on automatic control*, vol. 43, no. 4, pp. 475–482, 1998.

[8] P. R. Pagilla and B. Yu, "A stable transition controller for constrained robots," *IEEE/ASME Transactions on Mechatronics*, vol. 6, no. 1, pp. 65–74, Mar 2001.

[9] K. H. Johansson, M. Egerstedt, J. Lygeros, and S. Sastry, "On the regularization of zeno hybrid automata," *Systems & control letters*, vol. 38, no. 3, pp. 141–150, 1999.

[10] G. Ackerson and K. Fu, "On state estimation in switching environments," *IEEE Transactions on Automatic Control*, vol. 15, no. 1, pp. 10–17, 1970.

[11] A. Doucet, A. Logothetis, and V. Krishnamurthy, "Stochastic sampling algorithms for state estimation of jump markov linear systems," *IEEE Transactions on Automatic Control*, vol. 45, no. 2, pp. 188–202, 2000.

[12] U. Orguner and M. Demirekler, "Maximum likelihood estimation of transition probabilities of jump markov linear systems," *IEEE Transactions on Signal Processing*, vol. 56, no. 10, pp. 5093–5108, 2008.

[13] K. Youcef-Toumi and D. A. Gutz, "Impact and force control," in *IEEE International Conference on Robotics and Automation*, 1989, pp. 410–416.

[14] O. Khatib and J. Burdick, "Motion and force control of robot manipulators," in *IEEE International Conference on Robotics and Automation*, vol. 3, 1986, pp. 1381–1386.

[15] J. M. Hyde and M. R. Cutkosky, "Contact transition control: An experimental study," in *IEEE International Conference on Robotics and Automation*, 1993, pp. 363–368.

[16] S. S. M. Salehian and A. Billard, "A dynamical system based approach for controlling robotic manipulators during non-contact/contact transitions," *IEEE Robotics and Automation Letters*, pp. 1–1, 2018.

[17] G. E. Box, J. S. Hunter, and W. G. Hunter, *Statistics for experimenters: design, innovation, and discovery*. Wiley-Interscience New York, 2005, vol. 2.

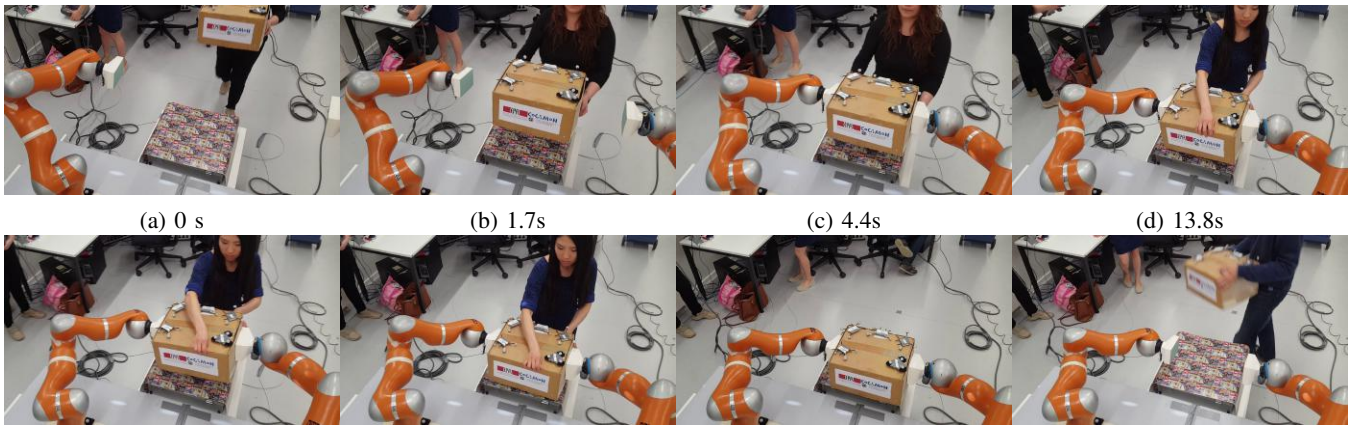

(a) 0 s (b) 1.7s (c) 4.4s (d) 13.8s

(e) 16.4s (f) 17.2s (g) 33.4s (h) 41.0s

Fig. 4: Snapshots of the robots' motion. In (a) and (b), the virtual object based motion generator guides the robots towards the moving object. In (c), the robots make secure contacts with the object. In (d), (e), (f), The robots remain in contact with the object even under external perturbations. In (g), the object is at a desired location, where a third operator hoists it as illustrated in (h). The corresponding video is available on-line: https://youtu.be/MZikIS-rSn4.

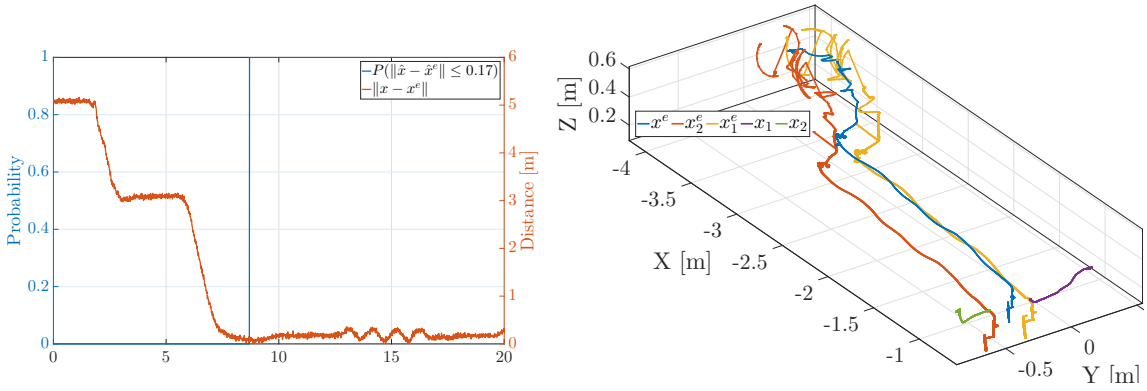

(a) (b)

Fig. 5: An example of the position of the object, the end-effectors and the probability of being in contact. The grabbing positions are specified by markers on the object. In order to track the object, all the markers must be feasible to cameras. However, the object's tracking was obscured partly by the robots when it is close to them. Hence, the measurements are not only noisy but also they might be wrong for some sampling times. Due to the implementation limitations, the markers are placed inside of the object and not on the sides. Hence, the distance between the measured grabbing positions on the object and the surface of the object is not zero and it is $17cm$. Therefore, $\delta = 0.17$.

[18] S. S. M. Salehian, N. Figueroa, and A. Billard, "Coordinated multi-arm motion planning: Reaching for moving objects in the face of uncertainty," in *Proceedings of Robotics: Science and Systems*, AnnArbor, Michigan, June 2016.

[19] ——, "A unified framework for coordinated multi-arm motion planning," *The International Journal of Robotics Research*, April 2018.

[20] H.-C. Lin, J. Smith, K. K. Babarahmati, N. Dehio, and M. Mistry, "A Projected Inverse Dynamics Approach for Multi-arm Cartesian Impedance Control," in *IEEE/RSJ Int. Conf. on Robotics and Automation*, 2018.

[21] F. Aghili, "A unified approach for inverse and direct dynamics of constrained multibody systems based on linear projection operator: applications to control and simulation," *IEEE Transactions on Robotics*, vol. 21, no. 5, pp. 834–849, Oct 2005.

[22] M. Mistry and L. Righetti, "Operational space control of constrained and underactuated systems," *Robotics: Science and systems VII*, pp. 225–232, 2012.

APPENDIX

A. Virtual object based controller

In the *free-space* phase, in order to coordinate the motion of the arms with each-other and with that of the object, we use the idea of the virtual object. Here, we briefly introduce the virtual object based motion generator. For more information, the readers are refereed to [19], [18].

The motion of the virtual object is generated by using the following dynamical system:

$$\ddot{x}^v = \frac{1}{3}\Big(\gamma\ddot{x}^e + 2\dot{\gamma}\dot{x}^e + \ddot{\gamma}x^e + A_2(\dot{x}^v - \dot{\gamma}x^e - \gamma\dot{x}^e) + A_1(x^v - \gamma x^e) + \sum_{i=1}^{2} U_i\Big) \tag{14}$$

where x^e and x^v are the states of the real and the virtual objects, respectively. $0 < \gamma < 1$ is the *coordination* parameter and of class C^1. The origin is located on the desired intercept point; i.e. $x^e(T^*) = \begin{bmatrix}0 & \dots & 0\end{bmatrix}^T$. U_i is the interaction effect of the tracking controller of the i^{th} end-effector on the virtual object:

$$U_i = \ddot{x}_i^d + A_{2i}^R(\dot{x}_i^v - \dot{x}_i) + A_{1i}^R(x_i^v - x_i) \tag{15}$$

where x_i is the current end-effector state, and x_i^d is the desired end-effector state calculated based on the tracking error between the i^{th} point on the virtual object and end-effector of the i^{th} manipulator:

$$\ddot{x}_i^d = \ddot{x}_i^v - A_{2i}^R(\dot{x}_i^v - \dot{x}_i) - A_{1i}^R(x_i^v - x_i) \tag{16}$$

To avoid any collision between the robots' body parts, the centralized IK solver proposed in [19] is used to convert the desired end-effector state (x_i^d) to the desired joint state (q_i^d).

In this phase, as the robots' motions are not constrained by the object, the contact force is not present: $F_c = 0$. Hence, the objective of the low-level controller is to asymptotically/exponentially track the desired motion generated by the virtual object (16); i.e.

$$\lim_{t\to+\infty} \|q - q^d\| = 0 \qquad \lim_{t\to+\infty} \|\dot{q} - \dot{q}^d\| = 0 \tag{17}$$

where $q = \begin{bmatrix}q_1 & q_2\end{bmatrix}^T$ and $q = \begin{bmatrix}q_1^d & q_2^d\end{bmatrix}^T$ are the real and the desired joint configurations, respectively. By defining $\tau = u_2(x, x^e, \varphi)$, where $u_2(x, x^e, \varphi)$ is the following joint-space impedance controller, (17) can be achieved.

$$\begin{aligned} u_2(x, x^e, \varphi) = M(q)(\ddot{q}^d - D_d(\dot{q} - \dot{q}^d) - K_d(q - q^d)) \\ + H(q, \dot{q}) \end{aligned} \tag{18}$$

In the aforementioned equation, D_d and K_d are diagonal positive definite matrices and φ is the state of the virtual object, and the joint configurations.

B. Projected inverse dynamic controller

While the robots are in the contact with the object, the constraints from the contact modify the motion of the robots, resulting the relation

$$\begin{aligned} (I - P)\dot{q} &= 0 \\ (I - P)\ddot{q} - \dot{P}\dot{q} &= 0 \end{aligned} \tag{19}$$

where $P = I - J_c^+ J_c$ is the projection matrix that projects an arbitrary vector onto the null space of the constraint J_c. By utilizing the technique proposed by [21], [22], The control law can be decomposed into two orthogonal components

$$\tau = \tau_u + \tau_c = P\tau + (I - P)\tau \tag{20}$$

where $\tau_u \equiv P\tau$ denotes the torque in the *unconstrained subspace* that controls the motion of the robot, and $\tau_c \equiv (I - P)\tau$ denotes the torque in the *constrained subspace* that maintains the the contacts. By projecting (13) into the null space of the constraints, one can write the projected dynamic of the robots as follows:

$$PM(q)\ddot{q} + PH(q, \dot{q}) = P\tau \tag{21}$$

As $PM(q)$ is rank-deficient, we cannot directly invert $PM(q)$ to calculate $\ddot{q}$. However, by utilizing the technique proposed by [21], [22], one can re-write (21) as follows:

$$(\underbrace{PM + I - P}_{M_c})(q)\ddot{q} + PH(q, \dot{q}) = P\tau \tag{22}$$

where M_c is a full rank matrix. Hence, (22) can be re-written as follows:

$$\ddot{q} = M_c^{-1} P(\tau - H(q, \dot{q})) \tag{23}$$

[20] proposed a constraint Jacobian for multi-arm manipulation

$$J_c = (I - G^+ G) \begin{bmatrix} J_1(q_1) & 0 \\ 0 & J_2(q_2) \end{bmatrix} \tag{24}$$

where G is the grasp matrix. By using J_c defined in (24), the projection $P = I - J_c^+ J_c$ decomposes the dynamic equation such that the unconstrained subspace handles the *external force* and the constrained subspace handles the *internal force* of the system.

$$\tau = u_1(x, x^e, \varphi) = Pu_1^u + (I - P)u_1^c \tag{25}$$

where φ includes the velocities of the robots and the object. In the aforementioned control law, u_1^u controls the robots' motions along the *unconstrained* direction with a Cartesian impedance controller

$$u_1^u = J^T \left[h_c + \Lambda_c \ddot{x}^d - D_d(\dot{x} - \dot{x}^d) - K_d(x - x^d)\right] \tag{26}$$

where $\Lambda_c = (JM_c^{-1}PJ^T)^{-1}$ is the Cartesian space inertia matrix, and $h_c = \Lambda_c(JM_c^{-1}(PH(q, \dot{q}) - \dot{P}\dot{q}) - \dot{J}\dot{q})$ is the Cartesian space Coriolis, centrifugal and gravitational force.

In (25), u_1^c controls the robots' motions along the *constrained* direction and calculated by solving the following constraint optimization problem to fine the minimum actuator torques needed to maintain all contacts while satisfying the unilateral, the friction cone, and moment constraints.:

$$\begin{aligned} \underset{u_1^c}{\text{minimise}}\ & u_1^{cT}(I - P)u_1^c \\ \text{subject to}\ & \lambda_z^i \geq 0 \\ & \mu\lambda_z^i \geq \sqrt{(\lambda_x^i)^2 + (\lambda_y^i)^2} \\ & \gamma\lambda_z^i \geq |\lambda_{m,z}^i| \\ & \delta x\lambda_z^i \geq |\lambda_{m,x}^i| \\ & \delta y\lambda_z^i \geq |\lambda_{m,y}^i| \end{aligned} \tag{27}$$

where $\lambda_x^i, \lambda_y^i, \lambda_z^i$ and $\lambda_{m,x}^i, \lambda_{m,y}^i, \lambda_{m,z}^i$ are the contact forces and moments along each axis for i^{th} robot, respectively. [20] shows that (27) can be solved without explicit knowledge of contact forces and moments, and hence no force/torque sensor is needed.